Field investigations of the Sugar gold prospect, Dawson Range, Yukon (NTS 115J/14 and 115J/15)

S.E. Bartlett
University of British Columbia

M.M. Allan[1]
Mineral Deposit Research Unit, University of British Columbia

E.N. Buitenhuis, T.R. Smith
Kaminak Gold Corporation

C.J.R. Hart
Mineral Deposit Research Unit, University of British Columbia

Bartlett, S.E., Allan, M.M., Buitenhuis, E.N., Smith, T.R. and Hart, C.J.R, 2016. Field investigations of the Sugar gold prospect, Dawson Range, Yukon (NTS 115J/14 and 115J/15). *In:* Yukon Exploration and Geology 2015, K.E. MacFarlane and M.G. Nordling (eds.), Yukon Geological Survey, p. 1-16.

ABSTRACT

The Sugar gold prospect, located 20 km southeast of the Coffee gold deposits in Yukon, is hosted in the mid-Cretaceous Dawson Range batholith, of which three mappable sub-units are recognized: a biotite hornblende quartz monzodiorite; a K-feldspar phyric hornblende biotite syenogranite; and a biotite hornblende diorite. Plutonic rocks are cut by steep, west to northwest-striking andesite dikes of uncertain age. Alteration and mineralized zones coincide with fault-fracture zones that are parallel and proximal to dikes and their margins. Alteration is characterized by an early phase of calc-sodic (albite-amphibole) and potassic (pervasive biotite and fracture-controlled K-feldspar) alteration and a later phase of silica flooding and sericite alteration. Gold mineralization is associated with disseminated sulphides in zones of silica flooding and with variably sheared veins of quartz-carbonate-arsenopyrite ± pyrite ± freibergite ± stibnite ± sphalerite. Late chalcedonic quartz-carbonate and ferroan carbonate veins mark the collapse of the hydrothermal system.

[1]*mallan@eos.ubc.ca*

INTRODUCTION

The Sugar gold prospect (Yukon MINFILE 115J 062) is a cluster of structurally-controlled gold occurrences located in the Dawson Range of west-central Yukon, approximately 20 km southeast of the 4.9 Moz Coffee Gold deposits (Yukon MINFILE 115J 110 and 111; Fig. 1). Sugar presents an opportunity to contribute to an emerging metallogenic framework for structurally-hosted gold mineralization in the Dawson Range, building on recent studies at the Coffee deposits (Wainwright *et al.*, 2011; Buitenhuis, 2014; Buitenhuis, *et al.*, 2015; MacKenzie *et al.*, 2014a,b), the Boulevard gold prospect (Yukon MINFILE 115J 052; McKenzie *et al.*, 2013) and the Moosehorn (Longline) gold deposit (Yukon MINFILE 115N 024; Joyce, 2002). The presence of significant porphyry-type mineralization at the Casino Cu-Au-Mo deposit, only 10 km to the southeast of Sugar (Fig. 1), emphasizes current uncertainties of whether gold in this area of the Dawson Range is orogenic (*i.e.*, non-magmatic fluid sources) or whether magmatism plays a role in the generation of gold-mineralizing fluids.

In 2011-2012, Kaminak Gold Corp. explored the Sugar prospect by trenching and diamond drilling 12 holes, following the identification and delineation of several gold-in-soil anomalies over an approximate 2 x 5 km area (Fig. 2). Exploration activities focused on two main zones of anomalous soil geochemistry, which will be referred to as "Sugar West" and "Sugar East" (Fig. 2).

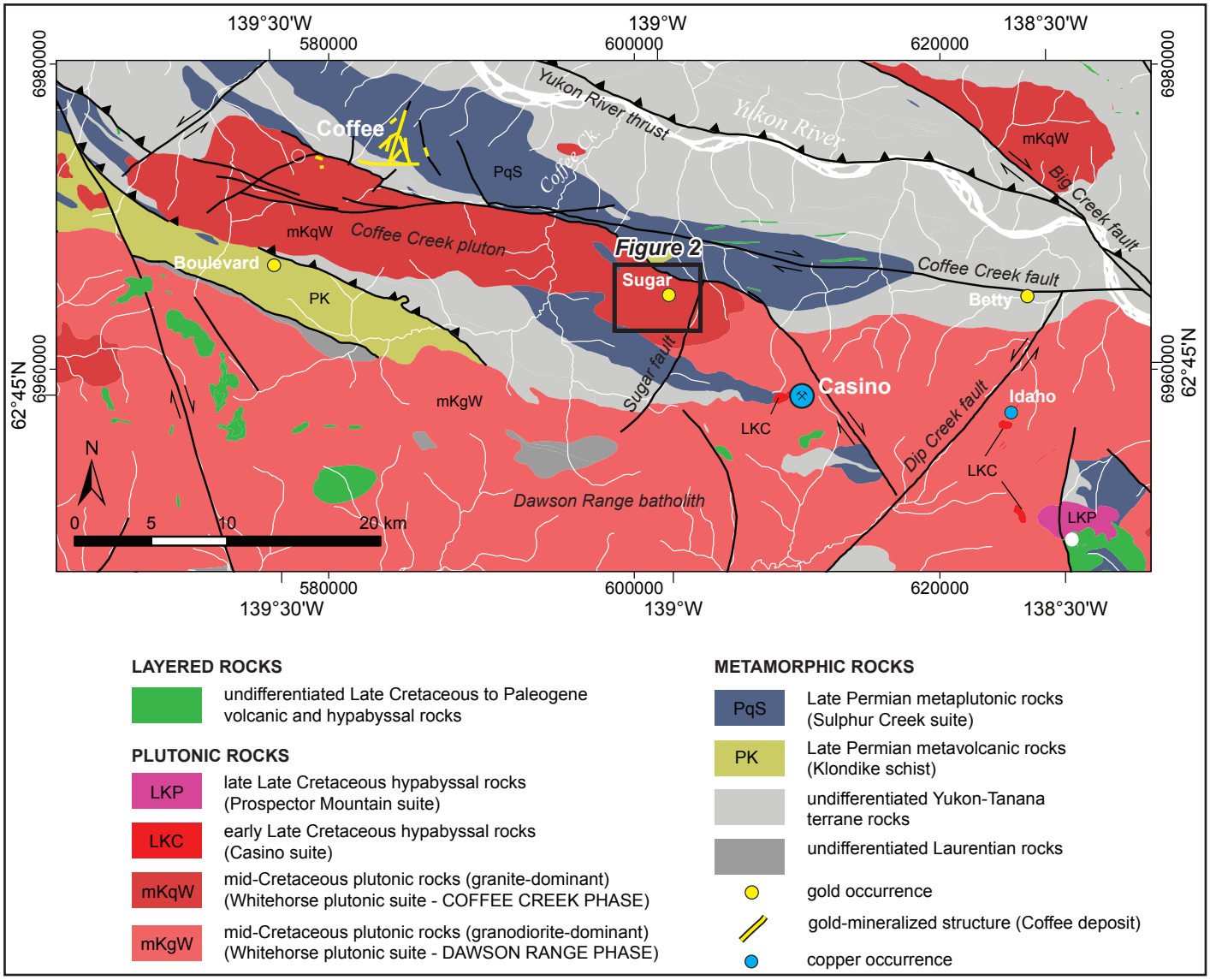

Figure 1. *Simplified regional geologic map of the western Dawson Range (Yukon Geological Survey, 2015), showing the location of the Sugar gold prospect relative to significant mineral occurrences.*

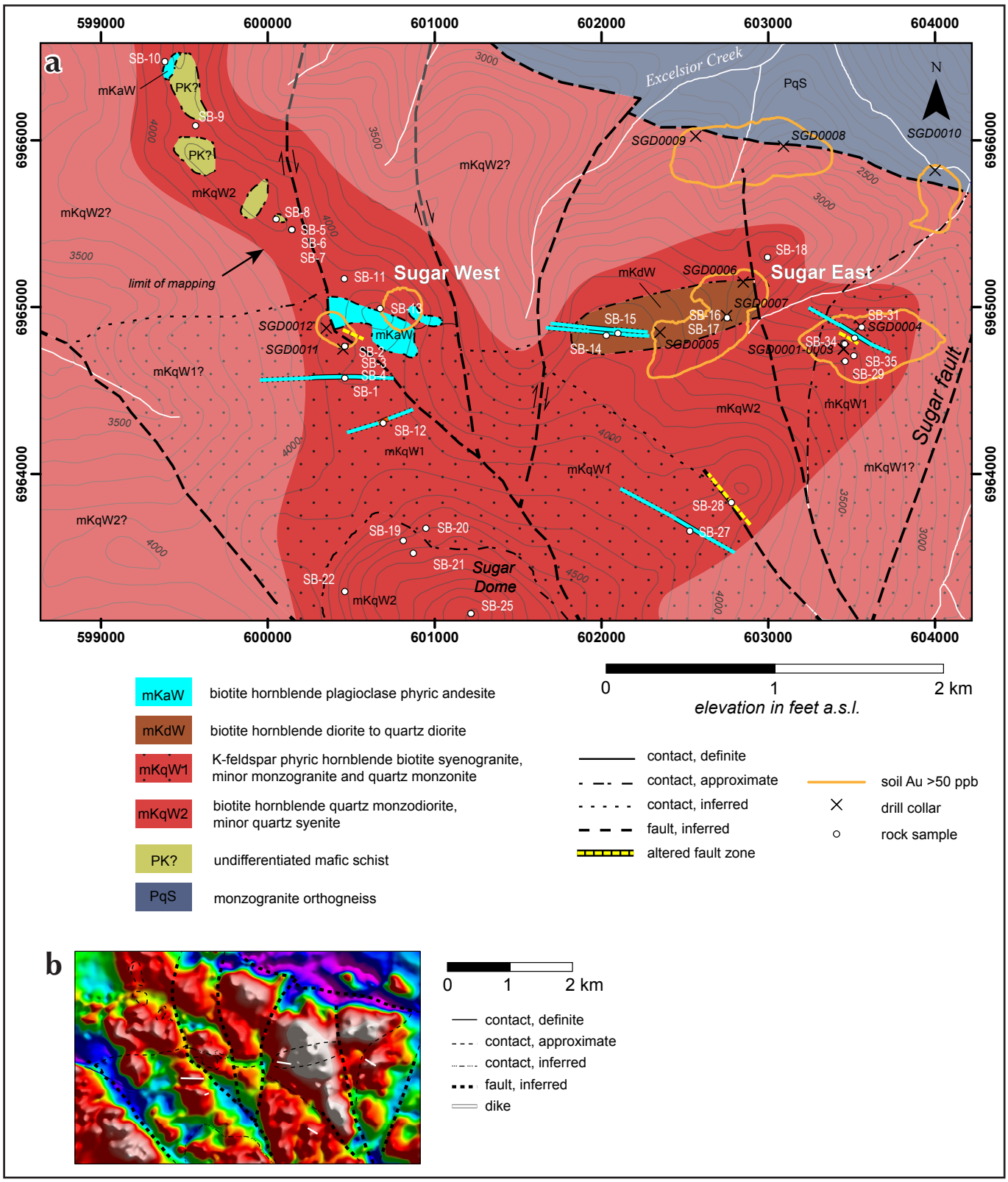

Figure 2. *(a) Geologic map of the Sugar gold prospect area based on 2015 fieldwork, with geology interpreted beyond the limit of mapping indicated by muted colours. Note that dike width is exaggerated for clarity; actual dike width is 2 to 5 m. (b) Total magnetic intensity grid of the Sugar prospect, showing position of geologic contacts and faults (same extent as Figure 2a).*

The Sugar area is on a gently north-dipping plateau at an elevation of 3500-4000 ft above sea level, and ~2 km north of the peak named "Sugar Dome" (~5200 ft; Fig. 2). The prospect drains north into Excelsior Creek, a left-limit tributary of the Yukon River. The terrain is dominated by frost-heaved felsenmeer covered by moss, lichen and low shrubs at higher elevations, and by colluvial cover and dense vegetation at lower elevations. Outcrop is limited to 4-5% of the land area, as determined by imagery analysis and field mapping. This study presents the geologic setting of the Sugar gold prospect based on 1:5000 scale geologic mapping and drill hole observations, and provides a preliminary assessment of the controls on mineralization.

REGIONAL GEOLOGIC SETTING

Gold mineralization at the Sugar prospect is hosted entirely in granitoid units of the Dawson Range batholith, a multi-phase continental arc plutonic complex of the mid-Cretaceous Whitehorse plutonic suite that intruded along the southern margin of the allochthonous Yukon-Tanana terrane in west-central Yukon (Fig. 1; Templeman-Kluit, 1974; Ryan *et al.*, 2013a,b). North of the Sugar prospect, Yukon-Tanana terrane metamorphic rocks are dominated by felsic to intermediate orthogneiss of the Late Permian Sulphur Creek plutonic suite (Figs. 1 and 2). The Sugar prospect is located ~5 km west of the mapped contact of the main Dawson Range phase of the batholith (mKgW; 112-100 Ma; Breitsprecher and Mortensen, 2004; Ryan *et al.*, 2013a,b) and the slightly younger and dominantly granitic Coffee Creek phase (mKqW; 100-99 Ma; McKenzie *et al.*, 2013; Ryan *et al.*, 2013a,b; Fig. 1).

The Sugar prospect is located ~5 km south of the west-northwest-striking, dextral strike-slip Coffee Creek fault system. The western, horse-tailing termination zone of this fault imparts a structural control on the Coffee gold deposits (Allan *et al.*, 2014a; Sanchez *et al.*, 2014). A prominent northeast-striking fault located ~2 km east of Sugar (Ryan *et al.*, 2013a), herein called the Sugar fault, parallels the normal to oblique sinistral-normal Dip Creek fault east of the Casino deposit (Fig. 1), and may have similar kinematics. North of the Sugar prospect, the Dawson Range batholith and metaplutonic rocks of the Sulphur Creek suite (PqS) are in inferred fault contact (Fig. 1; Ryan *et al.*, 2013a,b).

METHODS

Geologic map units were defined during 1:5000-scale field mapping, and have been correlated to regionally defined units (Fig. 2; Yukon Geological Survey, 2015). Thirty-five rocks samples and twenty-two drill core samples were collected for the purpose of petrographic analysis, lithogeochemistry and geochronology. Regional unit assignments will be confirmed by U-Pb geochronology. All rock names and descriptions have been based on modal mineralogy, verified by petrography and by digital image analysis of stained slabs (sodium cobaltinitrite for K-feldspar and amaranth red for plagioclase). In spite of the scarcity of outcrop, locally-derived felsenmeer provides confidence in the bedrock geology over much of the field area. The position of geologic contacts and faults in areas of cover were informed by Kaminak Gold Corp.'s total magnetic intensity and radiometric data, as well as topographic features such as slope breaks.

ROCK UNITS

The Sugar prospect is underlain primarily by the Coffee Creek phase of the Whitehorse plutonic suite (mKqW), of which two distinct, mappable subunits are identified: a K-feldspar phyric hornblende biotite syenogranite and minor monzogranite to quartz monzonite (mKqW1); and a compositionally and texturally heterogeneous unit dominated by biotite hornblende quartz monzodiorite, containing minor quartz syenite (mKqW2). The quartz monzodiorite contains locally abundant pebble to boulder-sized xenoliths of variably migmatitic, intermediate to mafic schist, which is interpreted as metavolcanic rocks of the Klondike Schist (PK) – the volcanic equivalent to metaplutonic rocks of the Sulphur Creek suite. Larger bodies of schist occur as rafts or roof pendants ~1 km northwest of Sugar West (Fig. 2). Volumetrically minor biotite hornblende diorite to quartz diorite (mKdW) forms a separate mappable body at Sugar East (Fig. 2). All units are cut by dikes of biotite hornblende plagioclase phyric diorite (mKaW), informally called "andesite" herein to differentiate it from the massive diorite unit mKdW.

More detailed rock unit descriptions are discussed below, in decreasing order of relative age. Mineralogical and textural descriptions in all cases are supported by petrographic observations of polished thin sections. Modal mineralogy and magnetic susceptibilities are included in Table 1.

BIOTITE HORNBLENDE QUARTZ FELDSPAR SCHIST (PK?)

This schist unit occurs as decimetre to metre-scale xenoliths within quartz monzodiorite of the Whitehorse plutonic suite (mKqW2). The schist also occurs as a ridge-forming series of coherent enclaves or roof pendants up to 300 m in length striking northwest from Sugar West (Fig. 2). The rock is typically fine-grained, grey-green and weathers dull brown to rusty red. Alternating sub-millimetre bands of biotite-hornblende and quartz-feldspar define a partially recrystallized metamorphic fabric. Locally discordant, undeformed granitic seams are also present, which are interpreted as a partial melt product (Fig. 3). Magnetic susceptibility of the unit is 9.0×10^{-3} SI units (Table 1).

The consistently fine-grained texture and intermediate to mafic composition of this schist unit, and its strike continuity with a large, mapped inlier of Sulphur Creek orthogneiss (Fig. 1; Ryan *et al.*, 2013b), suggests that it may be a metavolcanic equivalent, *i.e.*, Klondike Schist (PK).

BIOTITE HORNBLENDE QUARTZ MONZODIORITE TO QUARTZ SYENITE (mKqW2)

This unit forms topographic highs of outcrop and boulder talus, including Sugar Dome (Fig. 2). The unit varies from porphyritic to equigranular and from fine to coarse-grained (Fig. 4a), and contains up to 10% xenoliths of intermediate to mafic metavolcanic schist (PK?). The main lithology is a white-grey, hornblende biotite quartz monzodiorite, which is locally K-feldspar and plagioclase phyric and weathers brown-grey. The biotite commonly forms distinct euhedral, hexagonal grains, and is also interstitial with respect to phenocryst phases (Fig. 4b). The subordinate lithology is equigranular quartz syenite (Fig. 4c). Magnetic susceptibility of the unit ranges widely from 0.7 to 7.6×10^{-3} SI units (Table 1).

Table 1. *Selected samples from the Sugar gold prospect.*

Rock Unit	Sample	Northing (UTM Zone 7)	Easting (UTM Zone 7)	Modal Mineralogy	Magnetic Susceptibility ($\times 10^{-3}$ SI units)
mKaW	SB-01	600460	6964584	phenocrysts - 63% (plag - 33% hbl - 30%); matrix - 37%	19.6 ± 2.6 (n=6)
	SB-15	602097	6964853	phenocrysts - 25% (plag - 17% hbl - 5% bt - 3%); matrix - 75%	9.4 ± 2.5 (n=6)
	SB-30	603516	6964825	phenocrysts - 80% (plag - 50% hbl - 20% bt - 10%); matrix - 20%	10.7 ± 1.3 (n=6)
mKdW	SB-14	602027	6964840	qtz - 10%; plag - 60%; hbl -15%; bt - 15%	1.4 ± 0.4 (n=6)
	SB-17	602752	6964945	qtz - 2%; plag - 73%; hbl -17%; bt - 8%	7.3 ± 4.8 (n=6)
mKqW1	SGD0001_86.0m	603450	6964750	qtz - 15%; Kfs - 42%; plag - 34%; bt - 9%	5.9 ± 1.0 (n=6)
	SGD0011_38.0m	600450	6964750	qtz - 24%; Kfs - 45%; plag- 21%; hbl - 4%; bt - 6%	N/A
	SB-03	600461	6964775	qtz - 23%; Kfs - 36%; plag - 36%; bt - 5%	N/A
mKqW2	SB-06	600142	6965475	qtz - 15%; Kfs - 53%; plag - 26%; hbl - 3%; bt - 3%	0.7 ± 1.0 (n=6)
	SB-07	600142	6965475	qtz - 6%; Kfs - 20%; plag - 65%; hbl - 6%; bt - 3%	N/A
	SB-11	600457	6965180	qtz - 5%; Kfs- 23%; plag - 65%; hbl - 4%; bt - 3%	N/A
	SB-13	600672	6965001	qtz - 18%; Kfs- 47%; plag - 28%; hbl - 4%; bt - 3%	5.4 (n=1)
	SB-19	600811	6963610	qtz - 11%; Kfs- 21%; plag - 53%; hbl -10%; bt - 5%	N/A
	SB-24	601216	6963172	qtz - 10%; Kfs- 12%; plag - 45%; hbl -18%; bt - 15%	7.6 ± 4.8 (n=6)
PK?	SB-25	601291	6963038	qtz - 20%; Kfs- 15%; plag - 30%; hbl -20%; bt - 15%	9.0 (n=1)

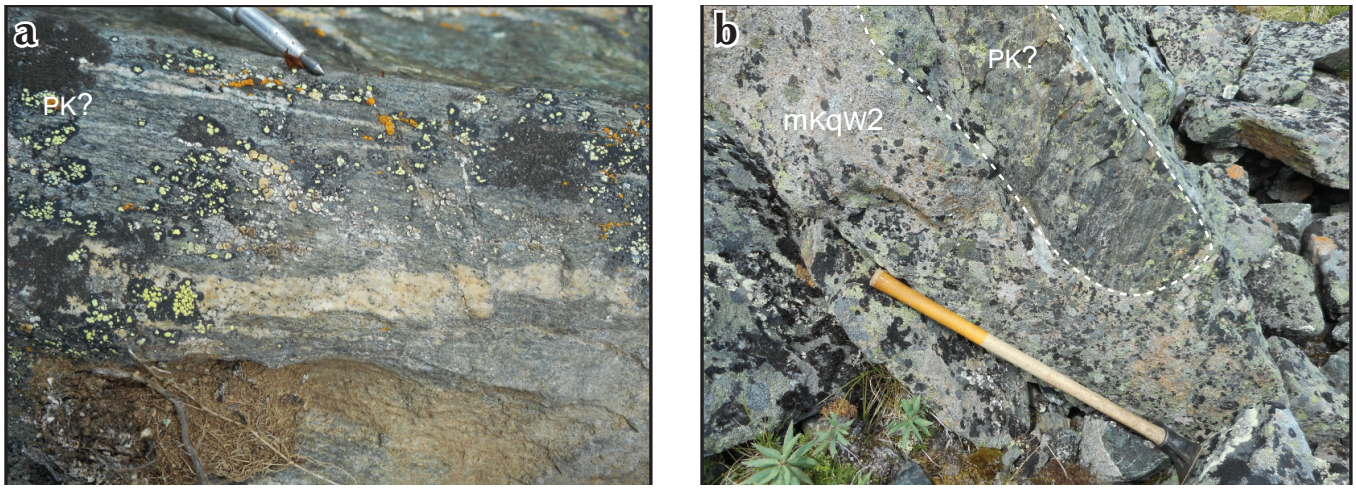

Figure 3. *Schist (unit* PK*?): (a) Xenolith of schist cut by a dikelet of granitic melt, interpreted as leucosome (pen-scribe for scale; Sample SB-9); (b) Xenolith of schist within quartz monzodiorite (*mKqW*2; Sample SB-25).*

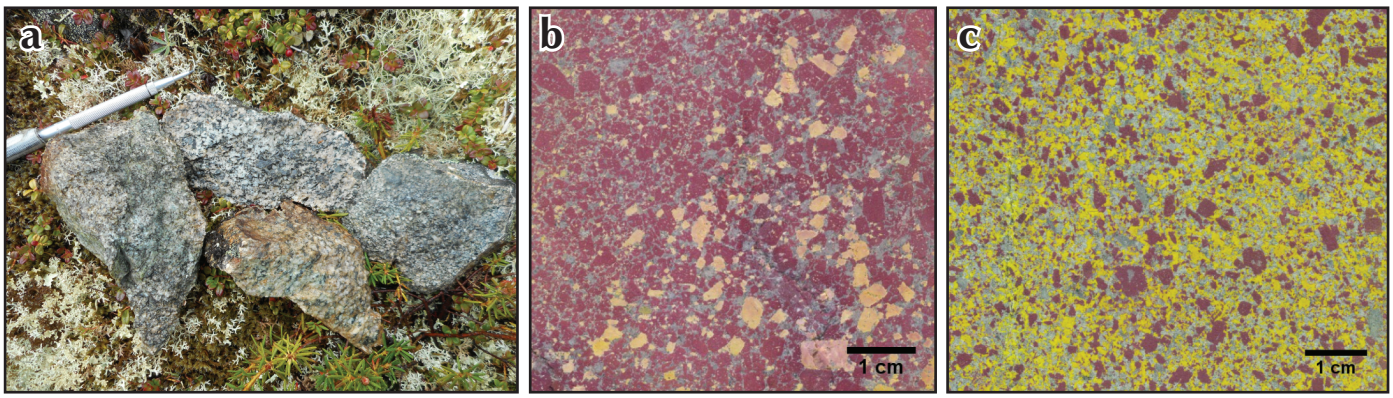

Figure 4. *Unit* mKqW*2: (a) Samples collected within a 10 m radius, indicating local heterogeneity (pen-scribe for scale; (b) Stained rock slab showing plagioclase and K-feldspar phyric quartz monzodiorite phase (Sample SB - 7) ; (c) stained slab showing quartz syenite phase (Sample SB-13).*

K-FELDSPAR PHYRIC HORNBLENDE BIOTITE SYENOGRANITE AND MINOR MONZOGRANITE TO QUARTZ MONZONITE (mKqW1)

This unit forms topographic lows and saddles and is observed mainly as float in frost-heaved felsenmeer, but also as rare outcrop near resistant andesite dikes (Fig. 5a). The unit has white-grey to chalky white weathering and contains smoky grey quartz. The unit is medium to coarse-grained and varies from equigranular to K-feldspar phyric. Plagioclase occurs interstitially to K-felspar phenocrysts and as euhedral laths in equigranular phases (Fig. 5b,c). Magnetic susceptibility of the unit is consistently ~6×10^{-3} SI units (Table 1).

BIOTITE HORNBLENDE DIORITE TO QUARTZ DIORITE (mKdW)

The diorite to quartz diorite unit intrudes granite (mKgW2) at Sugar East, and is cut by a porphyritic dike of similar composition ("andesite" below; Fig. 2). This rock unit is medium-grained and equigranular and contains subhedral plagioclase, hornblende and biotite (Fig. 6). In detail, biotite and hornblende grains are poikilitic with chadacrysts of plagioclase. Quartz content is variable, ranging from 0 to 10%. Magnetic susceptibility of the unit ranges from ~1 to 20×10^{-3} SI units (Table 1).

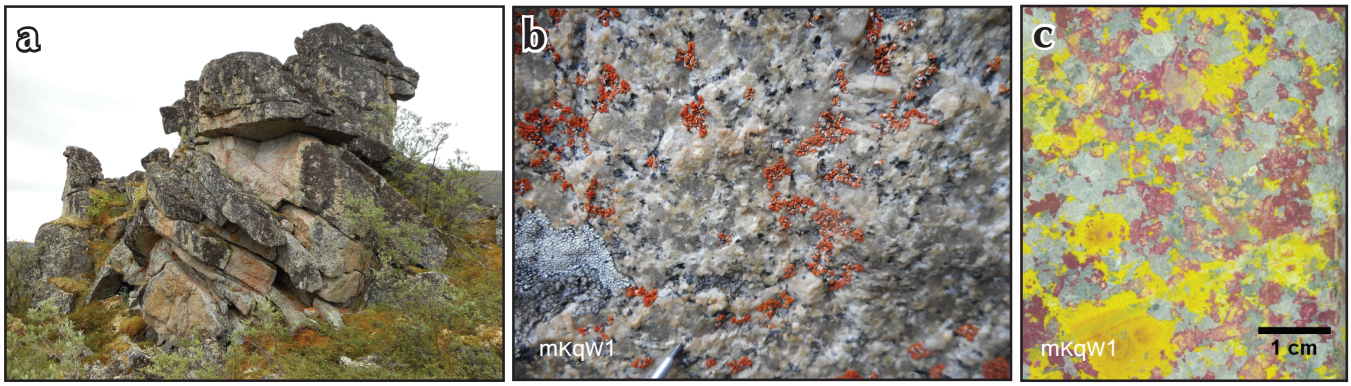

Figure 5. *Unit* mKqW*1: (a) Outcrop of granite exposed near resistant andesite dykes; (b) Representative K-feldspar phyric texture of syenogranite (pen-scribe for scale); (c) Stained slab of same granitic unit (from drill hole SGD0011).*

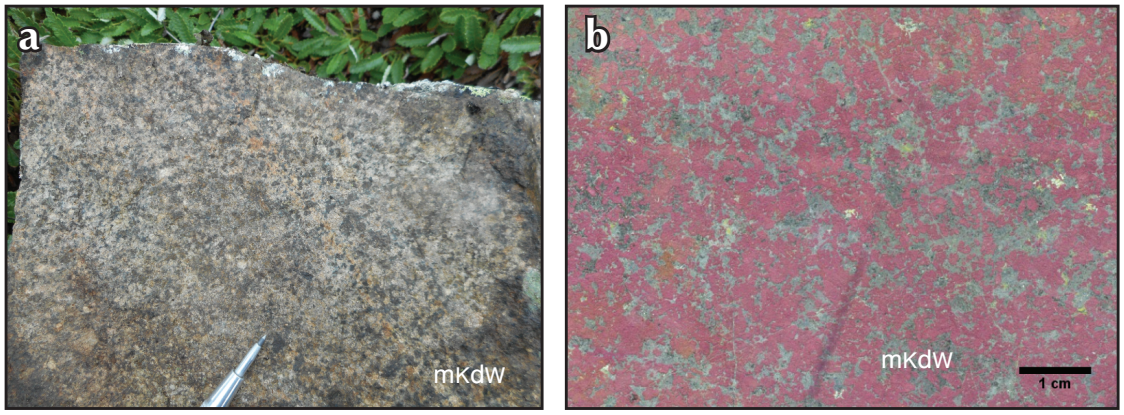

Figure 6. *Unit mKdW: (a) Biotite hornblende diorite float near drill hole (pen scratcher for scale; Sample SB-17); (b) Stained slab of biotite hornblende quartz diorite (Sample SB-14).*

BIOTITE HORNBLENDE PLAGIOCLASE PHYRIC DIORITE ("ANDESITE"; mKaW)

The unit is green-grey, weathers brown, and occurs mainly as subangular float and outcropping tors and ridges with subvertical fractures. This unit intrudes all other units as subvertical, west to northwest-striking dikes less than 10 m wide and as an irregular plug at Sugar West (Fig. 2). Intrusive contacts are subvertical and display a chilled margin of variable width (Fig. 7). Dike margins are also locally xenolithic with respect to more felsic host rocks.

Phenocryst abundance ranges from ~25% near dike margins to densely crowded (up to 90%) within dike interiors. Phenocrysts range from fine to coarse-grained with an average size of 2 to 5 mm. The groundmass is very fine-grained and comprises plagioclase, hornblende, and minor (less than 5%) quartz. This unit is magnetic (10 to 30 x 10^{-3} SI units) owing to its magnetite abundance. The unit is referred here informally as andesite, due to its porphyritic texture and to differentiate it from the equigranular phase (mKdW).

Figure 7. *Unit* mKaW*: (a) Andesite dike (*mKaW*) in contact with the more recessive syenogranite (*mKqW*1; near sample SB-1); (b) Chilled margin contact of porphyritic andesite with K-feldspar phyric syenogranite (pen-scribe for scale; near SB-12); (c) A stained slab of andesite (Sample SB-1).*

STRUCTURES

The main plutonic units (mKqW1 and mKqW2) are cut by an array of northwest to north-striking faults with apparent dextral displacement, as determined by offset geomagnetic markers in airborne magnetic data (Fig. 2b). Apparent dextral offsets on two such faults between Sugar West and Sugar East are each ~200 m. However, the timing of fault displacement relative to emplacement of the diorite and andesite units is unknown. These faults link to a southeast-striking fault that itself is a splay off the northeast-striking Sugar fault (Figs. 1 and 2).

Subvertical, hydrothermally altered fault-fracture networks occur parallel to, or coincident with, the west to northwest-striking andesite dikes and their margins (yellow dashed lines in Fig. 2a). Based on field and drillcore observations, these zones of deformation are 10s to 100s of metres wide, and are characterized by numerous individual brittle shears, fractures, veins and tectonic breccias. Three such structural corridors are recognized, and two of these are coincident with gold-in-soil anomalies (Sugar West and Sugar East, Fig. 2a). The third structural corridor is parallel to, but ~250 m north of, the andesite dike located ~1.5 km south of Sugar East. This structural corridor passes through a topographic saddle, which coincides with the intrusive contact between granite (mKqW1) to the south and quartz monzonite (mKqW2) to the north (Fig. 2a).

ALTERATION AND VEINING

Gold mineralization and both pervasive and fracture-controlled hydrothermal alteration are developed in the west to northwest-trending structural corridors described above. Pre, syn and post-mineralization veining and alteration are most intensely developed in granitoids, but also cross-cut andesite dikes. The broad spatial relationship between dikes, alteration and structural damage is evident both at Sugar West and Sugar East, as well as in a newly mapped dike and alteration zone about 1 km south of Sugar East (Fig. 2).

Because of the generally widely spaced, parallel nature of individual fractured, faulted, altered or mineralized features, some paragenetic relationships have not been observed. However, several important cross-cutting relationships establish the relative timing of magmatism, alteration and mineralization. These relationships are summarized in the paragenetic sequence shown in Figure 8, and each alteration type is described below and illustrated in Figure 9. Representative spatial relationships between dikes, veins, alteration types and mineralization are well illustrated by a graphical log of drill hole SGD0001 from Sugar East (Fig. 10).

GARNET-DIOPSIDE (EPIDOTE-CHLORITE)

Banded to massive andraditic garnet-diopside skarn-type alteration is observed overprinting xenoliths within quartz monzonite and syenogranite, and as endoskarn in immediately adjacent igneous rocks (Fig. 9a). Patchy epidote and chlorite occur as paragenetically later, overprinting alteration. The presence of calc-silicate alteration assemblages indicates a calcareous protolith, such as a calcareous member of the Snowcap assemblage (forming much of the undifferentiated Yukon-Tanana unit in Fig. 1), or potentially, a calcareous component of the Klondike schist, such as documented in the Klondike district (*e.g.*, Allan *et al.*, 2014b). The timing of this alteration relative to the timing of magmatism is unknown, but could have formed due to deuteric alteration from cooling and dehydration of the host granitoids, or by a subsequent magmatic-hydrothermal event.

EPIDOTE ± K-FELDSPAR

Epidote ± quartz ± pyrite veinlets (hairline to 2 cm wide) are observed exclusively in granitoid units, and are mantled by K-feldspar alteration haloes with a pink to brick-red hematite dusting. These veins have been cataclastically reworked with broken and randomly oriented feldspar grains cemented by epidote. Epidote-bearing veins occur both as single, widely spaced veins less than 0.5 cm wide, and as anastomosing swarms of hairline veinlets with locally pervasive K-feldspar alteration of the host granitoids (Fig. 9b). Cataclastically reworked epidote-chlorite veinlets cut andesite dike south of Sugar East; however, the timing of these veinlets relative to the epidote ± quartz ± pyrite veinlets is unknown.

AMPHIBOLE-ALBITE

Locally developed, pervasive, texturally destructive amphibole-albite alteration is observed overprinting K-feldspar phyric syenogranite proximal to a zone of garnet-diopside alteration in drill hole SGD0001 (Figs. 9c and 10). This style of alteration is manifested as albite replacement of pre-existing feldspar, and as fine-grained, dark green, randomly oriented amphibole overprinting mafic minerals. Rare vermicular amphibole-albite-pyrite veinlets with indistinct margins and albite haloes are observed in association with the pervasive albite-amphibole alteration (Fig. 9c). Alteration zones

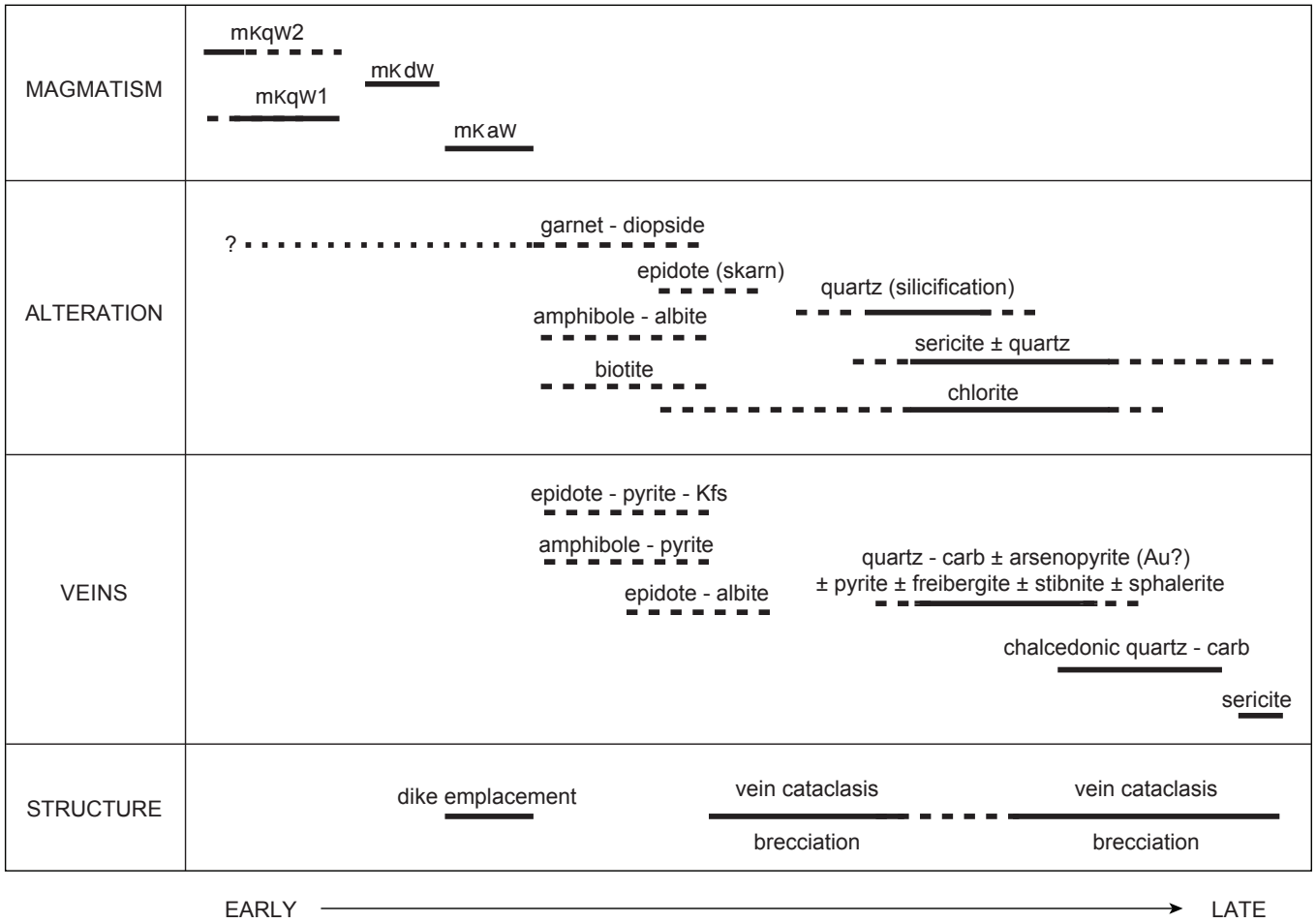

Figure 8. *Paragenetic scheme for magmatism, alteration, veining and structural activity at the Sugar prospect.*

are overprinted and obscured by silicification (Figs. 9c and 10) and by skarn-type epidote alteration (above). Therefore, the original extent of albite-amphibole alteration is unknown.

EPIDOTE-ALBITE

An epidote + albite assemblage is observed in hairline veinlets, cutting syenogranite (mKqW1) in drill hole SGD0001, along with albite-epidote alteration haloes in which albite replaces plagioclase rims (lower veinlet in Fig. 9c). Epidote in veins is subhedral and occurs in alteration haloes up to 1 cm wide.

BIOTITE

Biotite alteration is observed in porphyritic andesite in Sugar West (SGD0011) as an extremely fine-grained, pervasive and texturally destructive purple-brown overprint. This style of alteration is cut by fracture-controlled, chlorite and sericite alteration (Fig. 9d). The presence of biotite alteration in other localities has not been confirmed, and its timing relative to the epidote and albite-bearing alteration assemblages is uncertain (Fig. 8).

CHLORITE

Fracture-controlled chlorite alteration overprints hydrothermal biotite in andesite at Sugar West (Fig. 9d). Chlorite occurs as variably intense, patchy to pervasive alteration of magmatic biotite in granitic rocks distal to zones of silicification, sericitic alteration, brecciation and mineralization (Fig. 9e). However, the timing relationship of this chlorite alteration to these features is currently not well constrained.

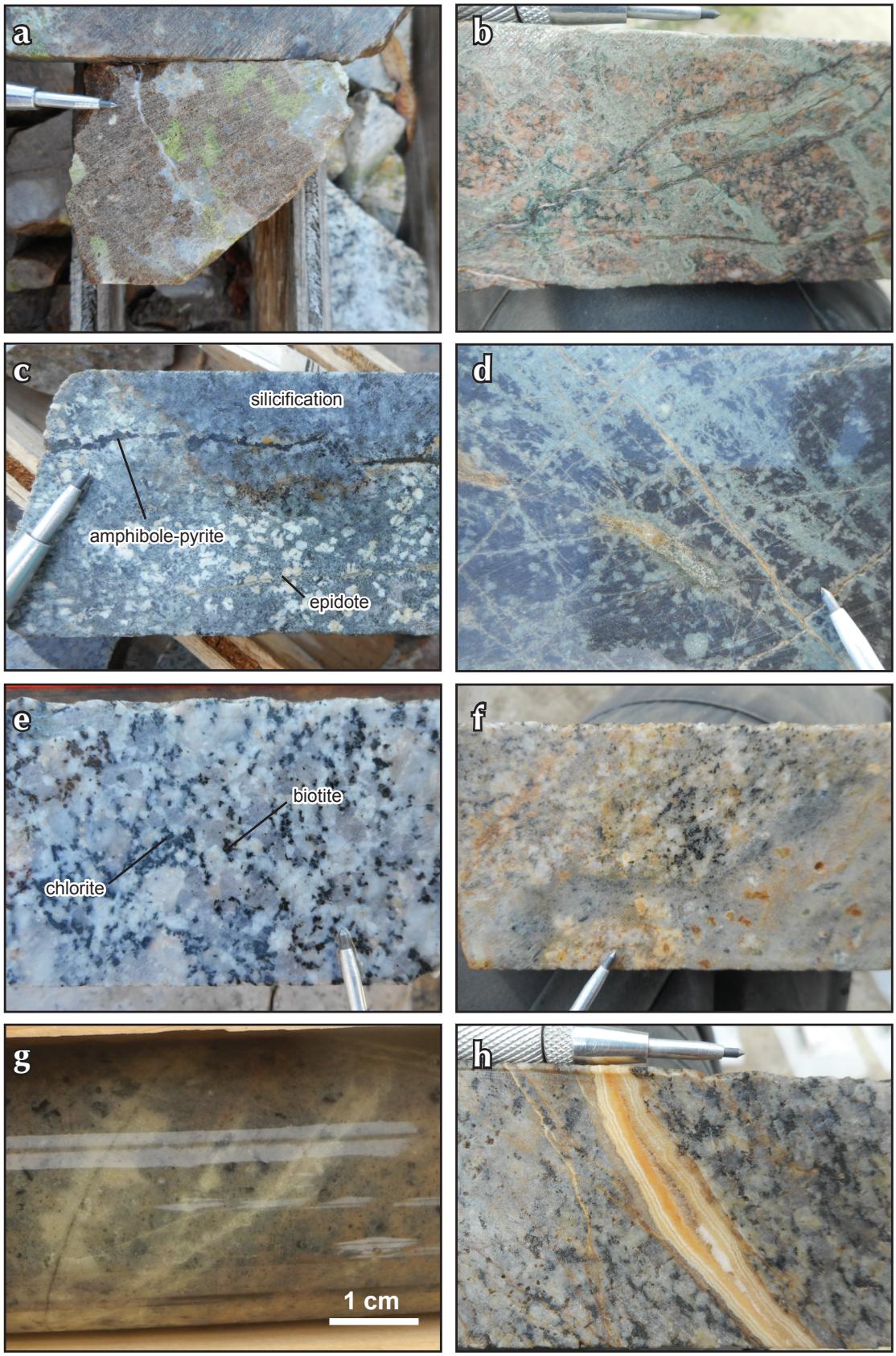

Figure 9. *Alteration styles of the Sugar prospect (pen-scribe for scale): (a) Andradite garnet-diopside-epidote skarn alteration of calcareous xenolith; (b) Wispy network of epidote veinlets with intense K-feldspar alteration cutting diorite; (c) Vermicular amphibole-pyrite veinlet with albitic halo (top) and hairline epidote vein with albite halo (bottom). Note the zone of cross-cutting silicification in the upper-right portion of the sample; (d) Pervasive biotite alteration of andesite, cut by fracture-controlled chlorite alteration (pale green) and later chalcedonic quartz-ferroan carbonate veinlets (orange); (e) chlorite alteration of magmatic biotite; (f) amoeboid front of silicification (bottom left) cutting granite (mKqW1); (g) fracture-controlled sericite alteration of previously silicified granite (note relict magmatic biotite); (h) laminated chalcedonic quartz -ferroan carbonate vein with late prismatic quartz and calcite cement.*

QUARTZ

Quartz alteration (*i.e.*, silicification) affects all rock units, including andesite dikes. It occurs as a mineralogically and texturally destructive alteration with sharp, digitate metasomatic fronts (Fig. 9f). Where silicification is intense, quartz completely replaces feldspar, but jagged, residual mafic grains are common. Silica flooding is common both in host granitoids and in andesite dikes, but is especially well developed in host rocks near dike margins (Fig. 10). Tectonic breccias not only contain clasts of silicified rock, but are overprinted by texturally destructive silicification, indicating that brecciation and silicification overlap paragenetically (Fig. 8). Zones of silicification overprint previously albite-amphibole altered rock (Figs. 9c and 10), and quartz replaces sericite-altered cores of plagioclase in both the syenogranite and quartz monzodiorite units.

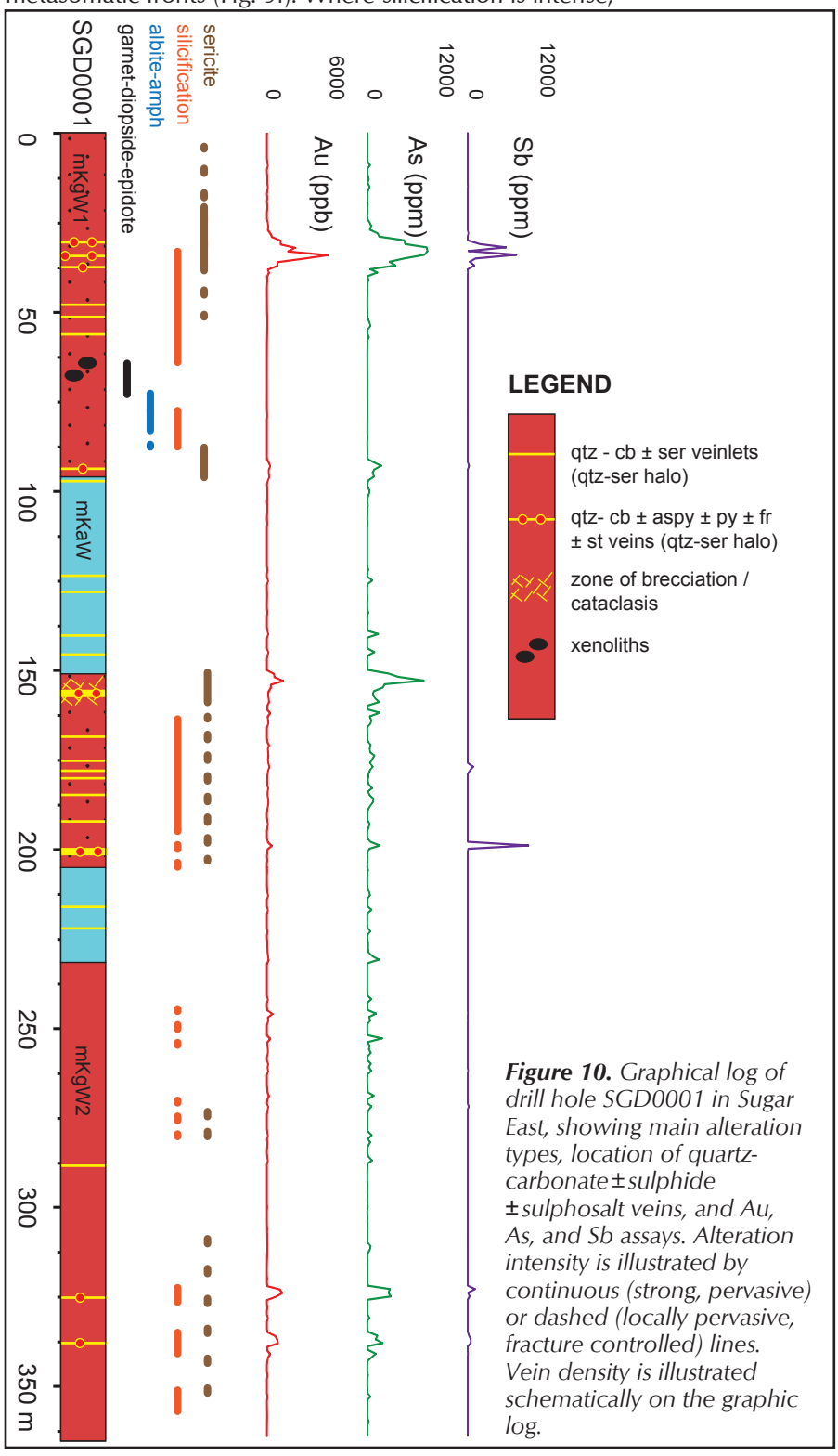

Figure 10. *Graphical log of drill hole SGD0001 in Sugar East, showing main alteration types, location of quartz-carbonate ± sulphide ± sulphosalt veins, and Au, As, and Sb assays. Alteration intensity is illustrated by continuous (strong, pervasive) or dashed (locally pervasive, fracture controlled) lines. Vein density is illustrated schematically on the graphic log.*

SERICITE

Biotite and feldspar-destructive sericitic alteration is observed as bleached haloes to both barren and mineralized quartz ± carbonate veins (see below), and clearly cross-cuts zones of silicification (Fig. 9g). Sericite also occurs in paragenetically late, hairline to 1 cm wide veinlets that cut silicified andesite and all other lithologic units. These sericite veinlets typically occur in anastomosing, variably oriented swarms.

CHALCEDONIC QUARTZ - FERROAN CARBONATE

Chalcedonic quartz-ferroan carbonate veins are observed cutting all lithologies and most alteration and vein types (Fig. 9h). Veins vary in width from hairline up to 2 cm. The hairline veins generally have ferroan carbonate concentrated along the vein margins, whereas the larger veins tend to contain sub-millimetre-scale laminations of chalcedonic quartz and ferroan carbonate, with paragenetically late, clear prismatic quartz and calcite in the vein centres (Fig. 9h). Chalcedonic quartz-ferroan carbonate veins cut zones of brecciation, but also occur as breccia clasts, suggesting that vein formation and brecciation were overlapping processes.

SECONDARY OXIDES

Sulphide-bearing zones are variably overprinted by scorodite and secondary limonite, but hypogene sulphides are preserved close to surface in all drill holes and trench exposures investigated.

ALTERATION SUMMARY

Following intrusion of the andesite dikes in the Sugar area (mKaW), hydrothermal features track a general paragenetic trend from (a) early, higher-temperature potassic (biotite) alteration of some andesite dikes, locally developed calc-sodic (albite-amphibole) alteration of host granitoids and garnet-diopside alteration of calcareous xenoliths, to (b) lower-temperature silicification, sericite alteration and variably gold-mineralized quartz-carbonate ± sulphide ± sulphosalt veins. Finally, cross-cutting chalcedonic quartz-ferroan carbonate veins and anastomosing sericite veinlets mark overprinting by the last, lowest-temperature part of the hydrothermal system.

MINERALIZATION

Gold mineralization confirmed by diamond drilling at Sugar occurs as 0.3 to 5 ppm anomalies over drill intercepts up to 10 m wide. Gold correlates strongly with arsenic in drill core assays and soil geochemistry over several orders of magnitude (Figs. 10 and 11a). Antimony is variably enriched in zones of anomalous gold, although the relationship is not strong (Figs. 10 and 11b). Zinc is also weakly anomalous in gold-mineralized zones, measuring enrichments up to several 100s of ppm compared to background levels below 100 ppm.

Gold grades correlate with occurrences of quartz-carbonate-arsenopyrite ± pyrite ± freibergite ± stibnite ± sphalerite veins and tectonic breccia cements (Fig. 12a-c). Freibergite ($(Ag,Cu)_{12}Sb_4S_{13}$) was identified as an important Sb-bearing phase as determined from Cu, Ag, Sb and S peaks in the energy-despersive X-ray spectra of three mineralized samples. The same sulphide-sulphosalt assemblage is present in the quartz-sericite alteration haloes to these veins (Fig. 12a). Mineralized features are overprinted by varying degrees of cataclastic reworking, as indicated by vein fragments in breccia zones and by shear-related microtextures.

In veins, freibergite and stibnite are interstitial with respect to quartz and carbonate, and arsenopyrite occurs as idiomorphic inclusions within freibergite and sphalerite (Fig. 12d). In disseminations proximal to veins, arsenopyrite is also idiomorphic (Fig. 12d). Gold was not observed during preliminary petrographic investigations by reflected light or scanning electron microscope.

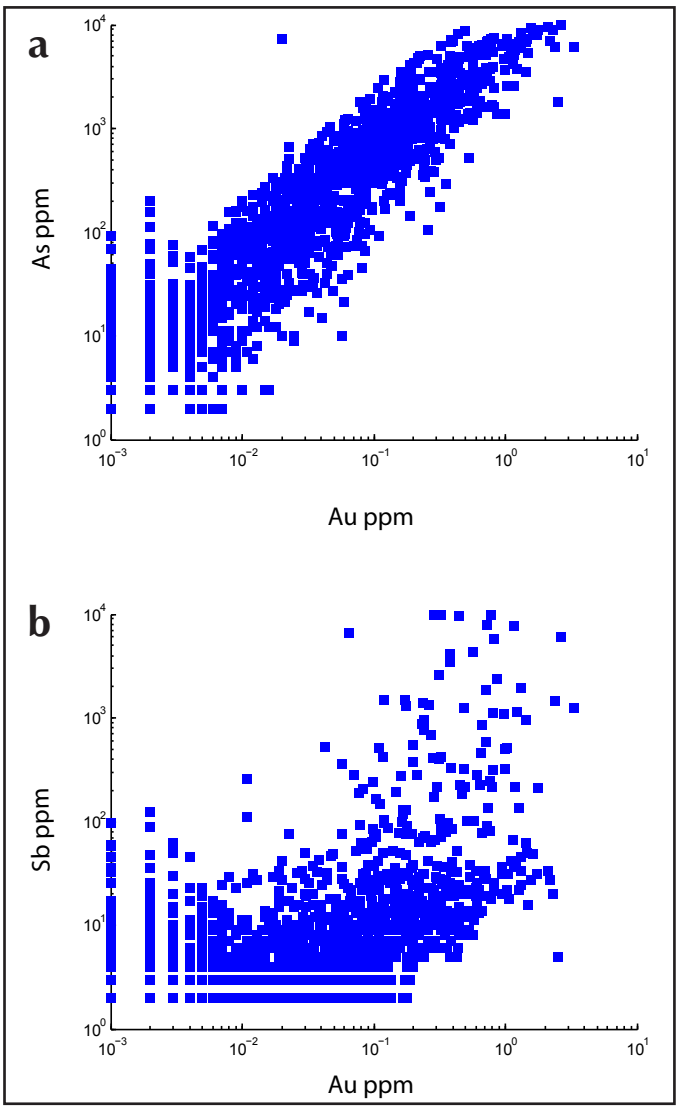

Figure 11. *Plots of (a) As vs. Au and (b) Sb vs. Au; from diamond drill hole assay data collected in 1 m intervals. The Au-As correlation is excellent over 3 orders of magnitude, whereas the Au-Sb relationship is erratic.*

Mineralization associated with cataclastic textures includes (a) 1 to 2 cm-wide veins of quartz and carbonate cementing clasts of granite, chalcedonic vein quartz and silicified rock, and (b) 1 to 3 m-wide zones of brecciation composed of granite clasts cemented by hydrothermal quartz and carbonate (Figs. 12b and 12c). Arsenopyrite within deformed veins shows grain size reduction and defines vein-parallel shear fabrics (Fig. 12e).

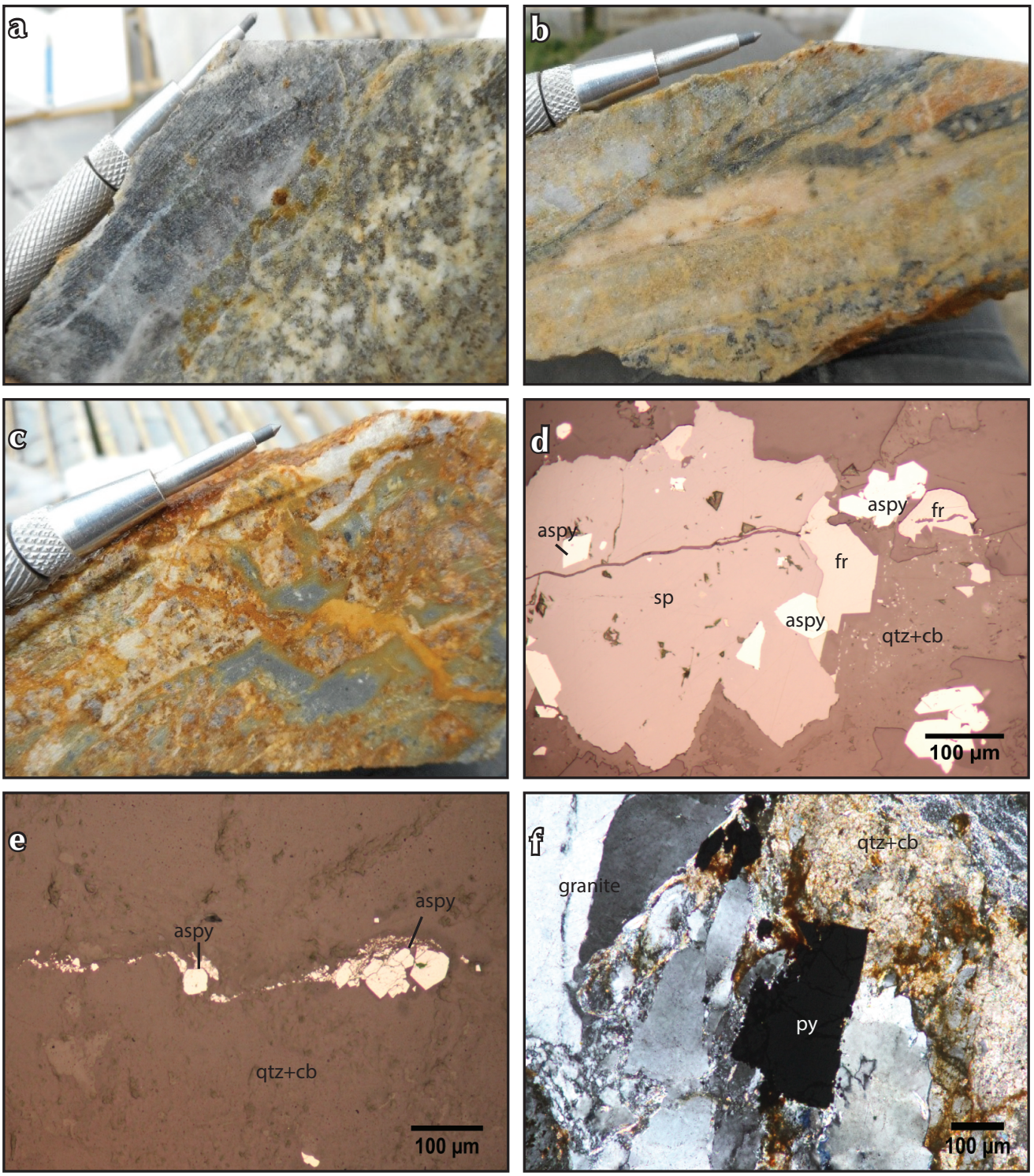

Figure 12. *Examples of mineralization styles at Sugar: (a) quartz-carbonate-arsenopyrite-freibergite-stibnite-sphalerite vein (left) with disseminated sulphides in the vein halo (right); (b) sheared quartz-carbonate-arsenopyrite-pyrite vein containing clasts of chalcedonic quartz and granite; (c) arsenopyrite-pyrite mineralized breccia with clasts of granite and chalcedonic quartz cemented by quartz and carbonate; (d) euhedral arsenopyrite (aspy) within a large anhedral sphalerite (sp) grain and blebbly, anhedral freibergite (fr) in a quartz (qtz) and carbonate (cb) matrix; (e) milled and sheared arsenopyrite grains within a deformed quartz-carbonate vein; (f) euhedral pyrite overprinting a granite clast in breccia.*

DISCUSSION

Gold mineralization at Sugar shares several features in common with mineralization at the Coffee gold deposits 20 km to the northwest. First, Sugar and Coffee share an obvious structural control, whereby mineralization is hosted in steeply dipping zones of brittle structural damage and no significant fault offsets are observed. The spatial and structural correlation of mineralization with andesitic dikes is also a common feature. Dikes are clearly pre-mineralization at Sugar due to local overprinting by silicification, quartz-carbonate veinlets, sericite alteration and mineralization. The same relative timing of dike emplacement and mineralization holds at Coffee. For both systems, dikes and hydrothermal features occupy the same structural corridors, suggesting that zones of structurally-enhanced permeability were active during both magmatic and hydrothermal episodes.

Second, both the Sugar prospect and Coffee deposits feature As and Sb anomalies coincident with Au mineralization, and the Au-As correlation is robust in both systems (Figs. 10 and 11). In hypogene sulphide ore at Coffee, most of the gold is present as solid solution in arsenian pyrite, whereas the main As-bearing phase at Sugar is arsenopyrite. This suggests that gold at Sugar is present either as solid solution in arsenopyrite, or as native gold in close paragenetic association with arsenopyrite.

Much of the mineralization at Coffee coincides paragenetically and spatially with structurally-controlled silicification (*e.g.*, Supremo zone; north-striking mineralization trends in Fig. 1). Silicification is also well-developed at Sugar, but is better characterized as proximal to mineralization, rather than having a direct genetic or spatial correlation (Fig. 10). Mineralization at Sugar is related to discrete veins (or vein breccias) of quartz-carbonate-arsenopyrite ± pyrite ± freibergite ± stibnite ± sphalerite, whereas mineralization is mainly disseminated at Coffee, and syn-mineralization veins at Coffee are rare.

Disseminated gold mineralization at Coffee is mainly associated with zones of illite-pyrite ± magnesian carbonate alteration of biotite-bearing host rocks. Carbonate is a ubiquitous gangue phase in mineralized veins and breccia zones at Sugar, but carbonate alteration of wallrocks has not been observed. Sericite (potentially illite) alteration is present at Sugar, and paragenetically overlaps with mineralization, but is mainly restricted to narrow zones of fracture-controlled alteration and is most closely associated with quartz alteration, rather than carbonate or pyrite. Whereas pyrite is abundant and closely correlated with gold mineralization at Coffee, it is a relatively minor sulphide at Sugar.

Weathering-related oxidation of pyrite along steep, mineralized structures at Coffee also played a key role in the formation of oxide facies gold mineralization. The relative lack of pyrite at the Sugar prospect has likely contributed to the poorly developed oxidation profiles. More aggressive uplift and erosion at Sugar may also play a role in the exposure of hypogene sulphides at surface.

The Sugar prospect's most significant deviation from the Coffee deposits is the presence of various high-temperature potassic and calc-sodic alteration types that pre-date mineralization. These include biotite alteration of andesite dikes, K-feldspar alteration associated with epidote veining, and albitization associated with secondary amphibole alteration of plutonic rocks. These alteration styles require high temperature and saline fluids typical of the porphyry environment. Although there is no mineralization associated with these early styles of alteration (except minor pyrite), their presence suggests the onset of a hydrothermal system shortly after, or related to, emplacement of the andesite dikes (Fig. 8).

Observations lead to the interpretation that Coffee and Sugar are broadly contemporaneous and probably genetically related hydrothermal systems on the basis of their similar structural control, Au-As-Sb association and common spatial and paragenetic relationships to andesite dikes. It is speculated that Sugar may represent a more deeply exhumed equivalent to the Coffee gold deposits, in which deeper-seated, higher-temperature alteration types and vein-controlled mineralization are exposed at the present-day erosional surface.

CONCLUSIONS

Sugar is a structurally-hosted gold system in which mineralization is tied spatially and temporally to brittle deformation along steep structures that are both proximal and parallel to mid-Cretaceous or younger andesite dikes. An early phase of calc-sodic and potassic alteration that overprints dikes and the immediate host rocks most likely signifies that a magmatic-hydrothermal system was active prior to, and potentially during, subsequent stages of silicification and gold-bearing quartz-carbonate-arsenopyrite ± pyrite ± freibergite ± stibnite ± sphalerite vein formation.

Of importance to the genetic and metallogenic interpretation of the Sugar gold prospect is the absolute timing of dike emplacement, potassic and calc-sodic alteration, and subsequent gold mineralization. Ongoing research will address the age of dikes and other magmatic phases by U-Pb dating of zircon, dating of alteration assemblages by Ar-Ar and gold deportment studies using scanning electron microscopy.

ACKNOWLEDGEMENTS

This study is the field component of a BSc Honours project by Stephen Bartlett at the Mineral Deposit Research Unit (MDRU) of the University of British Columbia, supervised by M. Allan. Helicopter-assisted fly-camp support and access to drill core was generously provided by Kaminak Gold Corp., and we are grateful in particular to Rory Kutluoglu, Geoff Newton, Adam Fage, Eric Buitenhuis and Tim Smith for technical discussions and enthusiastic logistical support. Financial support for the project was provided through the collaborative Kaminak-MDRU Yukon Coffee Gold Project, which is supported by NSERC CRD grant 474464-14. We are grateful to Farhad Bouzari for a constructive review of the manuscript.

REFERENCES

Allan, M.M., Sanchez, M.G., Mortensen, J.K. and Hart, C.J.R., 2014a. A hydrothermal record of structural overprinting and crustal exhumation in the White Gold District, Yukon. GSA Conference Abstract, Vancouver, BC, Oct 19-22, 2014.

Allan, M.M., Mortensen, J.K., and Cook, N., 2014b. Preliminary stable isotope and geochemical investigation of carbonate in the Klondike district. *In:* Yukon Exploration and Geology 2013, K.E. MacFarlane, M.G. Nordling and P.J. Sack (eds.), Yukon Geological Survey, p. 1-20.

Breitsprecher, K., and Mortensen, J.K. (compilers), 2004. Yukon Age 2004: A database of isotopic age determinations for rock units from Yukon Territory: Yukon Geological Survey (CD-ROM). Buitenhuis, E., 2014. The Latte gold zone, Kaminak's Coffee gold project, Yukon, Canada: geology, geochemistry, and metallogeny: Unpublished MSc thesis, University of Western Ontario, London, Ontario, 197 p.

Buitenhuis, E., Boyce, L. and Finnigan, C., 2015. Advances in the mineralization styles and petrogenesis of the Coffee gold deposit, Yukon. In: Yukon Exploration and Geology 2014, K.E. MacFarlane, M.G. Nordling and P.J. Sack (eds.), Yukon Geological Survey, p. 29-43.

Joyce, N.L., 2002. Geologic setting, nature, and structural evolution of intrusion-hosted Au-bearing quartz veins at the Longline occurrence, Moosehorn Range Area, west-central Yukon Territory. Unpublished MSc thesis, The University of British Columbia, Vancouver, Canada, 201 p.

MacKenzie, D., Craw, D. and Finnigan, C., 2014a. Lithologically controlled invisible gold, Yukon, Canada. Mineralium Deposita, vol. 50, p. 141-157.

MacKenzie, D., Craw, D. and Finnigan, C., 2014b. Structural controls on alteration and mineralization at the Coffee gold deposits, Yukon. In: Yukon Exploration and Geology 2013, K.E. MacFarlane, M.G. Nordling and P.J. Sack (eds.), Yukon Geological Survey, p. 119-131.

McKenzie, G.G., Allan, M.M., Mortensen, J.K., Hart, C.J.R., Sánchez, M. and Creaser, R.A., 2013. Mid-Cretaceous orogenic gold and molybdenite mineralization in the Independence Creek area, Dawson Range, parts of NTS 115J/13 and 14. *In:* Yukon Exploration and Geology 2012, K.E. MacFarlane, M.G. Nordling and P.J. Sack (eds.), Yukon Geological Survey, p. 73-97.

Ryan, J.J., Zagorevski, A., Williams, S.P., Roots, C., Ciolkiewicz, W., Hayward, N. and Chapman, J.B., 2013a. Geology, Stevenson Ridge (northeast part), Yukon. Geological Survey of Canada, Canadian Geoscience Map 116 (2nd edition, preliminary), scale 1:100 000, doi:10.4095/292407.

Ryan, J.J., Zagorevski, A., Williams, S.P., Roots, C., Ciolkiewicz, W., Hayward, N. and Chapman, J.B., 2013b. Geology, Stevenson Ridge (northwest part), Yukon. Geological Survey of Canada, Canadian Geoscience Map 117 (2nd edition, preliminary), scale 1:100 000, doi:10.4095/292408.

Sanchez, M.G., Allan, M.M., Hart, C.J.R. and Mortensen, J.K., 2014, Extracting ore deposit controlling structures from aeromagnetic, gravimetric, topographic, and regional geologic data in western Yukon and eastern Alaska. Interpretation, vol. 2, p. SJ75-SJ102.

Tempelman-Kluit, D.J., 1974, Reconnaissance geology of Aishihik Lake, Snag and part of Stewart River map-areas, west-central Yukon (115A, 115F, 115G and 115K). Geological Survey of Canada, Paper 73-41, 97 p.

Wainwright, A.J., Simmons, A.T., Finnigan, C.S., Smith, T.R. and Carpenter, R.L., 2011. Geology of new gold discoveries in the Coffee Creek area, White Gold District, west-central Yukon. In: Yukon Exploration and Geology 2010, K.E. MacFarlane, L.H. Weston and C. Relf (eds.), Yukon Geological Survey, p. 233-247.

Yukon Geological Survey, 2015. Yukon Digital Bedrock Geology, <http://www.geology.gov.yk.ca/update_yukon_bedrock_geology_map.html>, [accessed November 15, 2015].